U.P.B. Sci. Bull., Series B, Vol. 71, Iss. 3, 2009 ISSN 1454-2331

ORGANIC-INORGANIC MEMBRANE MATERIALS

Florina Daniela BĂLĂCIANU[1], Radu BARTOŞ[2], Aurelia Cristina NECHIFOR[3]

Sinteza silicei mesoporoase cu nanostructuri şi morfologii controlate a atras în ultimul timp atenţie deosebită datorită potenţialelor aplicaţii în cataliză, separări, transportul medicamentelor şi nanocompozite. Grupările organice ataşate pe materiale mesoporoase determină apariţia unor proprietăţi şi funcţii care nu se regăsesc la materialele anorganice. Lucrarea de faţă prezintă obţinerea pulberilor mesostructurate şi a filmelor subţiri de tip silice-C18. Acestea au fost caracterizate prin microscopie electronică, spectroscopie IR, determinarea suprafeţelor specifice şi a unghiului de udare.

The synthesis of mesoporous silica with controlled nanostructures and morphologies has received much attention owing to their potential applications in catalysis, separation, drug delivery and nanocomposites. Introducing organic groups in the mesoporous materials has attracted attention because the organic group has many varieties and peculiar functions that are not expected for the inorganic materials. In this paper, the preparation of silica-C18 mesostructured powders and thin films are presented. The powders and thin film were characterized by SEM microscopy, infrared spectroscopy, measurements of the specific surface area, and wetting angle measurements.

Keywords: organic-inorganic materials, silica, functional materials, nanoparticles, membranes

1. Introduction

The synthesis of mesoporous silica with controlled nanostructures and morphologies has been given much attention owing to their potential applications in catalysis, separation, drug delivery and nanocomposites.

Introduction of organic groups in the mesoporous materials have attracted attentions because the organic group has many varieties and peculiar functions that are not expected for the inorganic materials. Organic modification of the silicates permits precise control over the surface properties and pore sizes of the mesoporous sieves for specific applications, while at the same time stabilizes the

---

[1] Eng., PhD student, Department of Analitycal Chemistry and Instrumental Analysis, University POLITEHNICA of Bucharest, Romania

[2] Eng., PhD student, Department of Analitycal Chemistry and Instrumental Analysis, University POLITEHNICA of Bucharest, Romania

[3] Lecturer, PhD, Department of Analitycal Chemistry and Instrumental Analysis, University POLITEHNICA of Bucharest, Romania

materials towards hydrolysis. Bulk properties can also be affected by mixing organic and inorganic moieties in the mesostructures.

The inorganic components can provide mechanical, thermal, or structural stability, whereas the organic features can introduce flexibility into the framework, or change, for example, the optical properties of the solid. In the last few years, mesoporous solids have been functionalised in specific sites, and they proved to exhibit improved activity, selectivity and stability in a large number of catalytic reactions and sorption process. Mesoporous solids have been also examined for optical applications and as reactors or molds for polymerization processes.

For the preparation of silica particles we applied the polymeric route, using a molecular precursor, in our case TEOS (tetraethylorthosilicate).

Starting with homogeneous solution of soluble silica and octadecylurea triethoxysilane (C18) prepared in alcohol/water solvents, preferential evaporation of alcohol accompanying dip coating, it should drive silica/C18 self assembly into uniform or spatially patterned thin-film mesophases.

In this paper, the preparation of silica-C18 mesostructured powders and thin films are presented. The films were prepared using different compositions, with and without surfactants (CTAB and P123).

Various types of layers and synthetic methods can be distinguished: self supported thick layers obtained by interfacial reaction or by casting of gelling solutions, supported thin layers prepared by growth at the substrate-solution interface and by deposition of gelling solution. In the last case, silica layers exhibiting lamellar, hexagonal and cubic structures can be obtained.

In order to obtain thin layers we applied the dip coating techniques for the deposition of the sol obtained from silica and C18.

2. Experimental

2.1. Materials

Reagents

In the present work, the starting solutions were tetraethyl orthosilicate as silica source (TEOS, 98% Aldrich Chemicals Co.), ethanol (99,8 % Carlo Erba Reagents) and water-ethanol solution with ammonium hydroxide (28%, SDS). The reactants were used as received without any purification.

2.1.1. Synthesis of silica nanoparticles

The silica nanoparticles were synthesized following Stöber process, by controlled hydrolysis of TEOS in ethanol, using ammonia like a catalyst. [1, 2]

The hydrolysis was followed by condensation (polymerization) of the dispersed material. We followed two procedures presented bellow. All the experiments were performed at room temperature [1, 2].

Procedure 1

a). Silica nanoparticles

The particle growth reaction was initiated by mixing 5.64 g of ammonia (29% in massic procents) with 80 ml of ethanol. To this solution, 4.64 g of TEOS in 20 ml of ethanol, was added under stirring. After the complete addition of TEOS, the solution became cloudy in a few minutes. The stirring was maintained 2 hours. The final concentrations in the mixture were: 0.2 mol/l in TEOS, 2.0 mol/l in H_2O, 0.9 mol/l in NH_3 [3].

b). Acidification of the suspension

An aqueous 1M solution of HCl was added, under vigorous stirring, using a burette until a pH close to 2.

Procedure 2

14.1 g of H_2O and 10,6 g of ammonia (28 mass %) were mixed with 100 ml of ethanol. To this solution, 7 g of TEOS in 100 ml of ethanol was added under stirring. The solution became cloudy in a few minutes. The stirring was maintained 2 hours. The final concentrations in the mixture were of: 0.28 mol/l in TEOS, 10 mol/l in H_2O, 1.5 mol/l in NH_3. For some samples, we acidified the suspension until a pH close to 2.

In both cases, the suspensions were centrifuged at 5000 rpm for 20 minutes after stirring and acidification. The ethanol was removed and the particles were redispersed in acetone. The centrifuging-redispersing procedure was repeated for four times. After removing the acetone, silica powder was dried at 50°C for 4 hours.

2.2. Preparation of functionalized materials and devices

2.2.1. Preparation of grafted powders

Modification of silica surface relates to all the processes that lead to change in chemical composition of the surface. Surface can be modified either by physical treatment that leads to change in the ratio of silanol and siloxane concentration on the silica surface or by chemical treatment that leads to change in chemical characteristics of silica surface [4].

In order to graft C18, [3-(octadecyl)propil]ureatriethoxysilane, on the silica surface, we calculate the quantity of silica and the volume of solution of C18 necessary to obtain the grafting, using the values of specific surface obtained from nitrogen adsorption analysis. For example, for a specific surface of 5.2091 m^2/g, corresponds a volume of 100 ml solution 5×10^{-3} M of C18. The mixture was refluxed 12 hours, at 56°C.

The preparation of the C18 urea powders is outlined in Fig. 1:

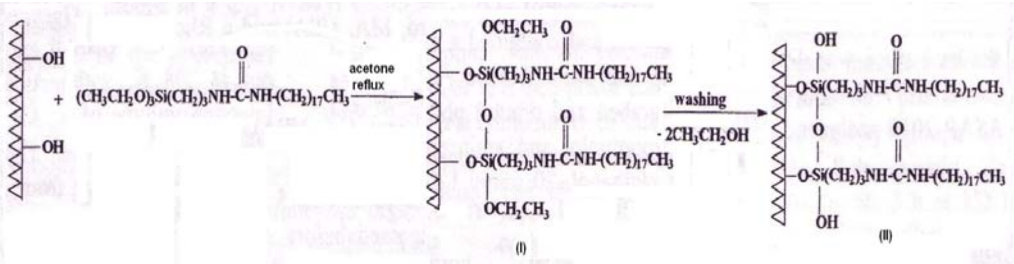

Fig. 1. Preparation of C18 urea-functionalized powders

Firstly, the urea-triethoxysilane was covalently attached to the powder surface (stepI). As described in Fig. 1, the ethoxy group which can be found on the powder surface is hydrolyzed during the washing procedure with acetone and ethanol, transforming into in more silanol groups (step II) [5-8].

2.2.2. Preparation of grafted membrane

Using the same principle like for the powders grafting, we carried out the experiment using 18 ml solution 5×10^{-3} M C18 in acetone for a zirconia membrane of 1 m^2 total surface. The membrane used it was a commercial one, supplied by INOCERMIC (Germany). The apparatus is shown in Fig. 2:

The **characteristics** of the membrane were:

- ☆ composed by:
  - ★support and intermediate layers: α-Al2O3.
  - ★top layer: zirconia, with the pore size of 3 nm.
- ☆diameter: ϕ = 47 mm; thickness: 1 mm

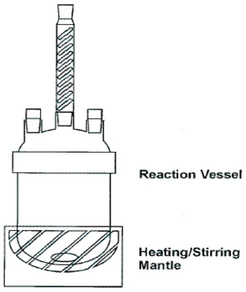

Fig. 2. Reaction apparatus for the grafting of zirconia membrane

2.2.3. Preparation of thin layers

For thin films preparing, the sol-gel technique is widely used. The property of the final gel can be varied both via the reaction conditions, and by incorporation of organic compounds in the SiO_2 structure. Such composite layers show a great variation of properties and can be used for a large field of applications [9-21].

In our work, the sol-gel systems were prepared via the two step method. The first step was mixing TEOS, acetone and an acidic aqueous solution with a pH close to the isoelectric point of silica (HCl, pH = 2) followed by a stirring period of one hour in order to obtain the prehydrolysis of TEOS. In the second step, to the solution prepared previously, different quantities of C18 dissolved in acetone were added and the stirring continued another 2 hours.

Table 1

Composition of the mixture employed to prepare nanostructured films

Crt. No.	TEOS mole	C18 mole	H_2O mole	HCl mole	$\phi\text{vol}=\frac{V_{C18}}{V_{C18}+V_{SiO2}}$
1	1	$2.65*10^{-4}$	2	$1.314*10^{-2}$	0.5
2	1	$2.65*10^{-4}$	1	$6.57*10^{-3}$	0.5
3	1	$2.65*10^{-4}$	0.5	$3.28*10^{-3}$	0.5
4	1	$2.65*10^{-4}$	0.05	$3.28*10^{-3}$	0.5
5	1	$3.172*10^{-6}$	2	$1.314*10^{-2}$	0.6
6	1	$2.65*10^{-4}$	1.5	$9.855*10^{-3}$	0.5
7	1	$3.869*10^{-4}$	2	$1.314*10^{-2}$	0.7
8	1	$3.869*10^{-4}$	1	$6.57*10^{-3}$	0.7
9	1	$3.095*10^{-4}$	1	$6.57*10^{-3}$	0.6
10	1	$3.095*10^{-4}$	0.5	$3.285*10^{-3}$	0.6
11	1	$3.095*10^{-4}$	0.55	$3.613*10^{-3}$	0.6

For the compositions from Table 1, the molar ratio between TEOS and acetone was 1/20.45:

$$\frac{\text{TEOS moles}}{\text{acetone moles}} = \frac{1}{20.45}$$

If we increase the volume fraction at $\phi_{vol} = 0.9$, and in this way the quantity of C18, it is necessary to use a bigger volume of solvent to dissolve this compound. The dilution increases and it is impossible to obtain a gel.

Using the same composition like the one from Table 3, but with different molar TEOS:acetone ratios, inhomogeneous thin layers were obtained:

$$\frac{\text{TEOS moles}}{\text{acetone moles}} = \frac{1}{4.8}$$

In order to obtain mesostructured layers we changed the precursor of silica (TMOS = tetramethoxysilane, MTES = methyltriethoxysilane or MTMS = methyltrimethoxysilane = instead of TEOS). The compositions are presented in the Tables 2 - 5.

Table 2

Compositions of thin layers (I)

Nr.crt.	TMOS moles	C18 moles	H_2O moles	HCl moles	$\phi vol = \frac{V_{C18}}{V_{C18} + V_{SiO2}}$
*12	1	$2.65*10^{-4}$	2	$1.314*10^{-2}$	0.5
13	1	$2.65*10^{-4}$	1	$6.57*10^{-3}$	0.5
14	1	$2.65*10^{-4}$	0.5	$3.28*10^{-3}$	0.5
15	1	$2.65*10^{-4}$	2	$1.314*10^{-2}$	0.5
16	1	$2.65*10^{-4}$	1.5	$9.855*10^{-3}$	0.5

Table 3

Compositions of thin layers (II)

Nr.crt.	MTES moles	C18 moles	H_2O moles	HCl moles	$\phi vol = \frac{V_{C18}}{V_{C18} + V_{SiO2}}$
17	1	$2.65*10^{-4}$	2	$1.314*10^{-2}$	0.5
18	1	$2.65*10^{-4}$	1	$6.57*10^{-3}$	0.5

Table 4

Compositions of thin layers (III)

Nr.crt.	MTMS moles	C18 moles	H_2O moles	HCl moles	$\phi vol = \frac{V_{C18}}{V_{C18} + V_{SiO2}}$
19	1	$2.65*10^{-4}$	2	$1.314*10^{-2}$	0.5
20	1	$2.65*10^{-4}$	1	$6.57*10^{-3}$	0.5

In the next experiences we decided to use two types of surfactants: cetyltrimethyl- ammonium bromide purchased from Sigma-Aldrich (CTAB) [22] and triblock copolymer poly(ethylene oxide)-poly(propylene oxide)-poly(ethylene oxide) EO20PO70EO20 (P123 from BASF France and labelled P123 [23, 24].

Table 5

Compositions of thin layers (IV)

Nr.crt.	TEOS moles	C18 moles	H2O moles	HCl moles	CTAB moles	P123 moles
21	1	$6.6*10^{-4}$	8.22	$5.34*10^{-2}$	0.81	-
22	1	$9.74*10^{-4}$	6.06	$3.97*10^{-2}$	-	2.39*10-3

The sols obtained were deposed as thin layers on flat glass substrates by dip coating [25]. The glass slides were degreased previously with a laboratory detergent, repeatedly rinsed with distilled water and then with acetone. To dip coat a film, the slides were immersed to a depth of 2 cm into the reaction mixture, allowed to stand for 1 minute and then withdrawn with a speed of 5 cm/min. The resulting films were dried at room temperature to preserve the porosity of the films.

The schemes of a dip coating process are shown in Fig. 3.

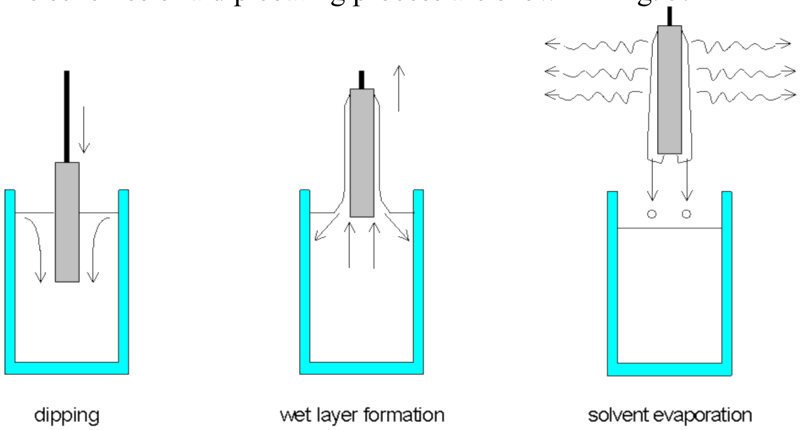

Fig. 3. Stages of the dip coating process: dipping of the substrate into the coating solution, wet layer formation by withdrawing the substrate and gelation of the layer by solvent evaporation

The nitrogen adsorption/desorption analyses for silica and zirconia samples were performed using an ASAP 2010 Accelerated Surface Area and Porosimetry System from MICROMERITICS. The ASAP 2010 system consists of an analyzer, a control module (computer), and an interface controller.

IR spectroscopy analyses were carried out on a Nexus (Smart Golden Gate, ATR Diamond) from Thermo-Nicolet.

The macroscopic morphology and quality of the powders and films were assessed by scanning electron microscopy (SEM) using a Hitachi S-4500 scanning electron microscope.

3. Results and discussion

3.1. Surface characterization

3.1.1. Nitrogen adsorption measurements

BET method was used for the measurements of the specific surface area [26]. The method consist in the determination of the volume of gas physical adsorbed at the surface of the material as a function of the relative pressure of the gas P/Ps (where P is the equilibrium pressure of the gas used, and Ps the saturate vapor pressure), at a given temperature T. Prior to BET analysis, the powders were degassed at 150 °C for 2 h under N_2 atmosphere to remove water trapped to the particle surface.

The pore size distribution was estimated by analysis of the adsorption and desorption curves using BJH method and assuming cylindrical pores [27].

In Table 6 are presented the principal properties of silica obtained from the adsorption/desorption isotherm.

Table 6

Properties of SiO_2 powder obtained from adsorption/desorption isotherm

Samples	**SBET (m^2/g)**	**BJH adsorption cumulative pore volume (cm^3/g)**	**BJH desorption cumulative pore volume (cm^3/g)**
PA12	5.2091±0.0571	0.010767	0.010832
PA13n	14.7515±0.3307	0.024634	0.025246

Two typical adsorption/desorption isotherms of the samples prepared using procedure 2, with and without neutralization of the suspension, are presented in Fig. 4 and Fig. 5, respectively.

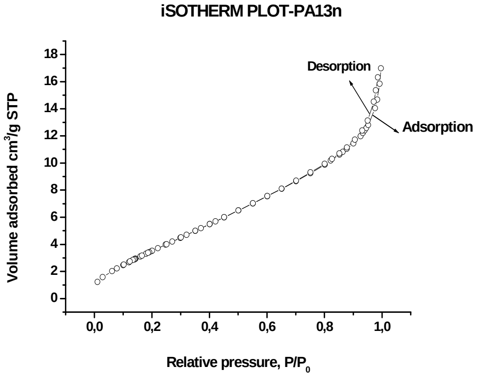

Fig. 4. Adsorption/desorption isotherm for silica sample PA13n, with neutralization

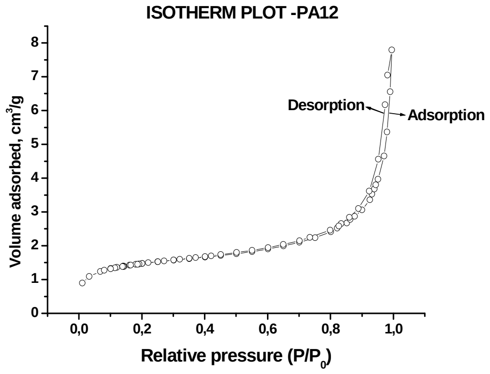

Fig. 5. Adsorption/desorption isotherms for silica sample PA12, without neutralization

The isotherms obtained for the samples of silica were found to be of type II according to the Brunauer, Deming, Deming and Teller (BDDT) classification that confirms the presence of a significant amount of macropores [28]. The same conclusion can be taken if we compare the BET surface area [29] (5.2091 m^2/g

±0.0571 m^2/g) and of the BJH adsorption cumulative surface area of samples pores (2.3290 m^2/g) – for sample PA12)-Fig. 6 and Fig. 7.

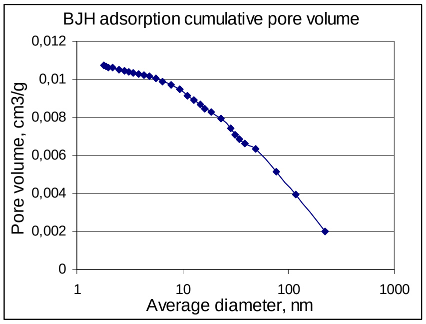

Fig. 6. BJH adsorption cumulative pore volume - sample PA12

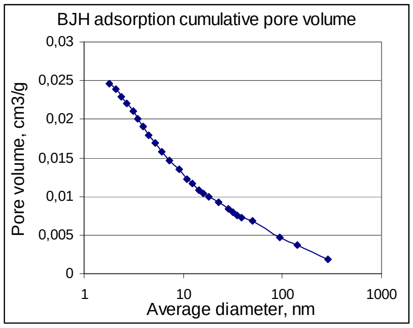

Fig. 7. BJH adsorption cumulative pore volume - sample PA13n

The adsorption cumulative pore volume was deduced to be 0.010767 cm^3/g. This corresponds to a porosity of 2.31 %, when a density of the silica matrix of 2.2 g/cm^3 was considered. The value of the porosity was deduced using next formula [29]:

$$\textbf{\textit{Porosity}} = \frac{\textbf{\textit{pore volume}} * \mathbf{100}}{\textbf{\textit{pore volume}} + \dfrac{\mathbf{1}}{\rho_{SiO_2}}}$$

3.1.2. Analysis of grafted solids by infrared spectroscopy

The chemical formula and the IR spectra of the compound that was grafted on the powders, labelled C18 (octadecylurea-propil triethoxysilane) are presented in Fig. 9.

$$(CH_3 - CH_2 - O)_3 - CH_2 - CH_2 - CH_2 - NH - CO - NH - (CH_2)_{17} - CH_3$$

labelledC18

The spectral assignments of C18 are presented in Table 7:

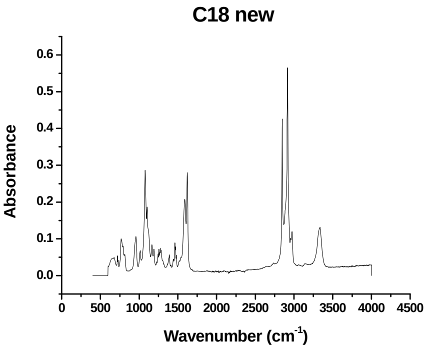

Fig. 8. IR spectra of C18

Frequency (cm-1)	Position assignment
482,00	
1260	
1588,97	
1626,14	-NH sec
2848,96	
2918,19	
3344,30	
669,44	(-CH2-)
1080,40	Si-O
1103,27	
1260	CH3-Si
1390,41	
1466,28	d-CH2
2848,96	
1390,41	CH3-CH2-
1390,41	d C=O
2918,19	-CH3

Table 7. Assignment of IR spectral data of C18

The IR spectra of pure silica and pure zirconia are presented in Fig. 9 and Fig. 10.

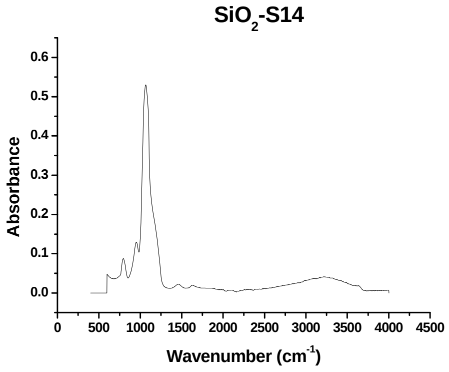

Fig. 9. IR spectra of SiO_2

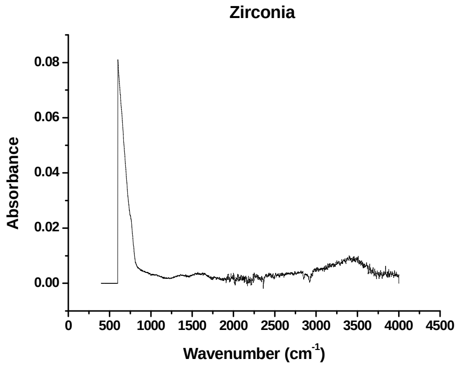

Fig. 10. IR spectra of zirconia

The IR spectral assignments of silica are shown in Table 8:

Table 8

Assignment of IR spectral data of silica

Frequency (cm^{-1})	**Position assignment**	**Literature value [30]**
797.7	O-H bending (silanol)	870-800
953.33	Si-OH bond stretching	980-935
1063.5	Asymmetric Si-O-Si stretching in S104 tetrahedron	1115-1050
1580	O-H bending (molecular water)	1625
3000-3500	O-H stretching and molecular water	3000-3800

Presence of adsorbed water and free surface silanol groups as well as siloxane linkages can easily be conceived from the IR spectra of silica in the range 400-4000 cm^{-1} which corresponds to the fundamental stretching vibration of different hydroxyl groups. The broadness of this band suggests different hydroxyl local environments of the OH groups. The band from 1580 cm^{-1} is assigned to the deformation mode of water molecules, which are probably trapped inside the voids. In the range 400-1500 cm^{-1} the spectrum has several bands. Thus, bands located at 797.9 and 1063.5 cm^{-1} are the bond bending and bond stretching vibration of Si-O-Si units [30].

Mixtures with different mass ratios were prepared in order to see how it should look the IR spectra of SiO_2 and zirconia grafted with C18.

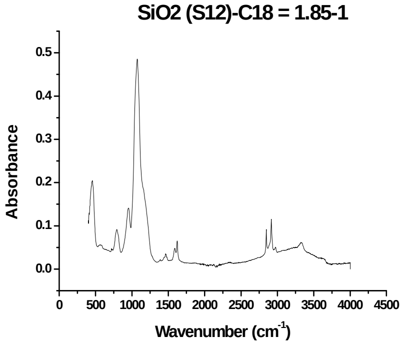

Fig. 11. IR spectra of the mixture SiO_2:C18=1.85:1 (mass ratio)

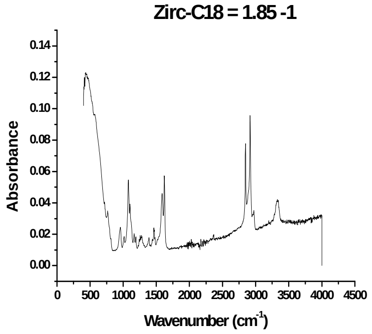

Fig. 12. IR spectra of the mixture zirconia:C18=1.85:1 (mass ratio)

The powders were analyzed by IR spectroscopy in order to determine the grafting of C18 on the surface of silica and zirconia. The IR spectra of the grafted powders are presented in Fig. 14 and 15:

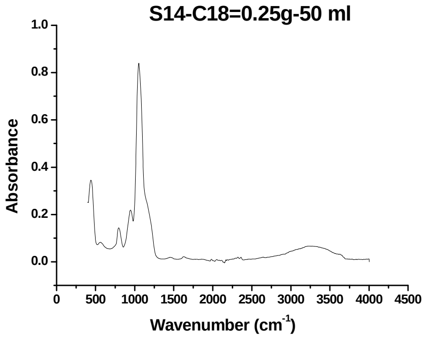

Fig. 14. IR spectra of silica grafted with C18 (0.25 g SiO_2 at 12.5 ml solution $5*10^{-3}$ M C18)

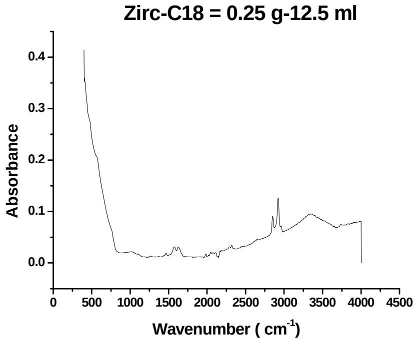

Fig. 15. IR spectra of zirconia grafted with C18 (0.25 g zirconia at 12.5 ml solution 10^{-3} M C18)

The IR spectrum of ZrO_2-C18 shown in Fig. 15, exhibited four peaks at 1572.66 cm^{-1} (-NH sec), 2853.47 cm^{-1} (for -NH sec and d–CH_2), 2923.37 cm^{-1} (for –NH sec and –CH_3) and 3327.24 cm^{-1} (-NH sec) which is similar to that of C18, confirming the existence of this compound on the surface of the membrane.

In case of grafting C18 on SiO_2, the IR spectrum (Fig. 14) shows that the reaction does not take place.

Assignments of IR spectral data of C18 on zirconia powder are presented in table 9:

Table 9

Assignments of IR spectral data of C18 on zirconia powder

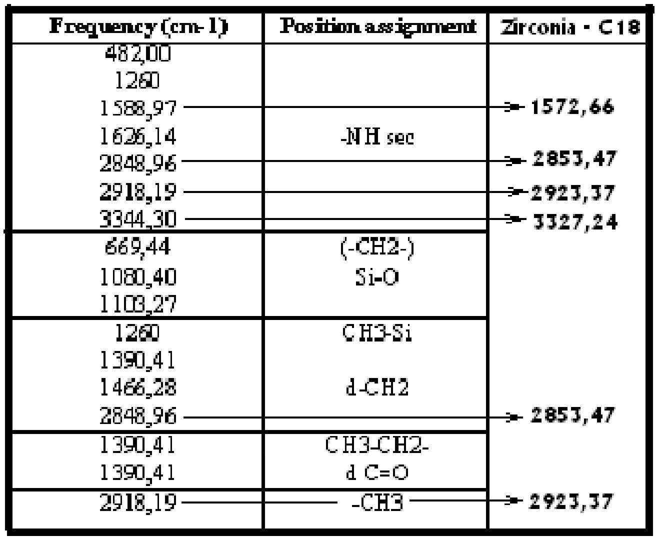

Frequency (cm-1)	Position assignment	Zirconia - C18
482,00		
1260		
1588,97		1572,66
1626,14	-NH sec	
2848,96		2853,47
2918,19		2923,37
3344,30		3327,24
669,44	(-CH2-)	
1080,40	Si-O	
1103,27		
1260	CH3-Si	
1390,41		
1466,28	d-CH2	
2848,96		2853,47
1390,41	CH3-CH2-	
1390,41	d C=O	
2918,19	-CH3	2923,37

3.1.3. Wetting angle measurements

Wetting of a surface is controlled to indicate a change in surface chemistry or topography. Contact angle measurements are often used to asses such changes of surface tension. The technique is based on the three-phase boundary equilibrium described by Young's equation:

$$\gamma_{LV}\cos\theta = \gamma_{SV} - \gamma_{SL},$$

where γ_{ij} is the interfacial tension between phases *i* and *j*, with subscripts corresponding to liquid, vapor and solid phase, respectively, and θ referring to the equilibrium contact angle (Fig.16) [31, 32].

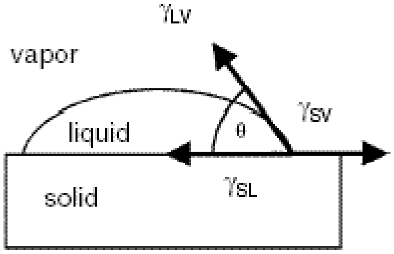

Fig. 16. Contact angle: definitions of interfacial tensions [16]

When water is the liquid, hydrophilic surfaces are characterized by a small contact angle. Young's equation applies to a perfectly homogeneous atomically flat surface.

Contact angle measurements were performed in order to control the efficiency of the grafting treatment with C18 of the zirconia membrane and to compare it to that obtained before the grafting. Different solvents with big surface tensions were used. The results are schematically presented in Table 10:

Table 10

Experimental data obtained for contact angle measurements

Zirconia membrane	**Contact angle**		
	Solvent		
	water	Ethylene glycol	Benzaldehyde
Without grafting	45°	33°	5°
Grafted with C18	76°	76°	56°

The values of the angles show a clear difference between grafted membrane and the one without grafting.

This type of analysis was the only one that showed the presence of C18 on the surface of the membrane. The results of the other methods that we used (IR, RAMAN) were not convincing. One of the reasons could be that the layer of C18 deposed on the membrane was too thin.

3.1.4. Morphology of the powders and layers by SEM

The morphologies of the powders of silica (without and with neutralization of the suspension) are presented in Fig.s 17 and 18. The particles of silica obtained using procedure 2, with acidification of the suspension, are more aggregated and bigger then the particles obtained without acidification.

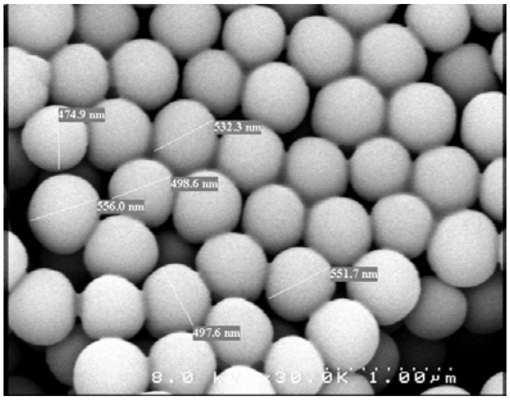

Fig. 17. SEM micrograph of silica obtained using procedure 2 without acidification of the suspension

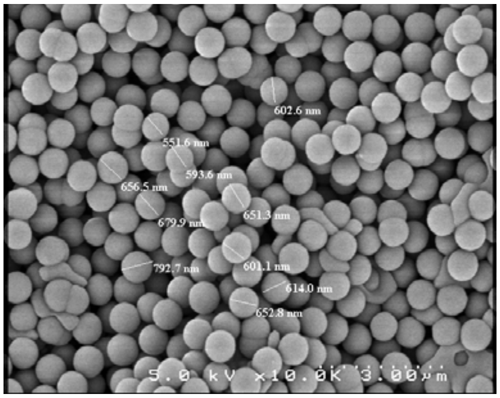

Fig. 18. SEM micrograph of silica obtained using procedure 2 with acidification of the suspension

Using the compositions from tables 2-5, we obtained thin layers by deposition on flat glass substrates by dip-coating (e.g. Fig. 19-22).

The thickness was not homogeneous across the films. It is clear, that even at relatively high values of TEOS molar ratio water: unhydrolyzed monomers can be present in the gel [33]. The results of this incomplete hydrolysis for the film is that, after coating, the hydrolysis continues during the drying process, giving rise to a continuously evolving microstructure which leads to a gradual decrease in the film thickness. The hydrolysis continuation was facilitated by exposure to moisture in the atmosphere.

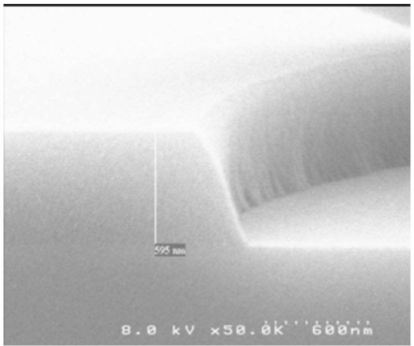

Fig. 19. The thickness of the layer obtained from C18 and CTAB as surfactant

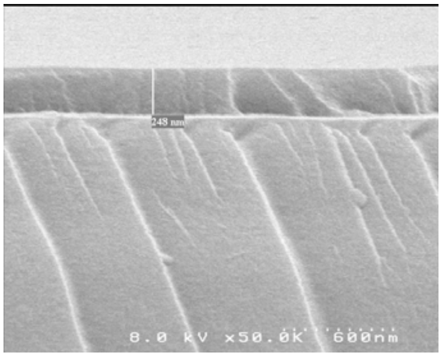

Fig. 20. The thickness of the layer obtained from C18 and P123 as surfactant

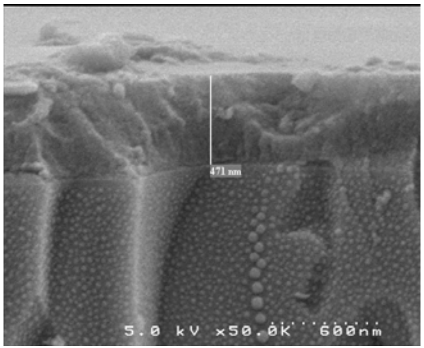

Fig. 21. The thickness of the layer obtained from C18 and TMOS as precursor of silica

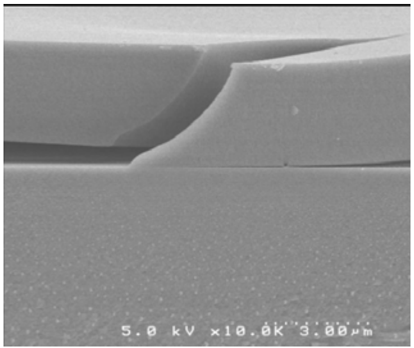

Fig. 22. Thin layer obtained after calcinations at 400°C/4 hours

4. Conclusions

In the present work, a new organic compound, octadecylurea triethoxysilane (C18), was grafted on the surface of silica and zirconia nanoparticles.

The polymeric route was applied for the preparation of silica nanoparticles using a molecular precursor, in our case TEOS (tetraethylorthosilicate).

The same procedure was followed for a zirconia membrane. The studied powders and membrane were analyzed by SEM, IR, small angle X-ray diffraction and contact angle.

The results obtained using IR analysis of the zirconia powder show a clear evidence of the grafting of organic compound. For silica the grafting did not occur.

Contact angle measurements were performed in order to control the efficiency of the grafting treatment of the zirconia membrane with C18 and to compare it with that obtained before the grafting. This type of analysis was the only one that evidenced the presence of C18 on the surface of the membrane. The results of the other methods that were used (IR, RAMAN) were not convincing.

In what concerns the preparation of silica-C18 thin films, the thickness of the films were not homogeneous all the time. Most of the films obtained do not diffract. This result was associated to a preferential alignment of the micellar cylinders parallel to the substrate plane.

REFERENCES

[1] *W. Stöber, A., Fink, E. Bohn*, "Controlled growth of monodisperse silica spheres in the micron size range"**,** in J. Colloid Interface Sci., **vol. 26**, issue 1, January 1968, pp. 62-69

[2] *D.L. Green, J.S. Lin, Yun-Fai Lam, Dale W. Schaefer, M.T.Harris*, "Size, volume fraction, and nucleation of Stober silica nanoparticles", in J. Colloid Interface Sci., **vol. 266**, issue 2**,** 2003, pp. 346-358

[3] *L.A. Belyakova, A.M. Varvarin,* "Surfaces properties of silica gels modified with hydrophobic groups", Coll. Surf. A: Phys. Eng. Asp., **vol. 154**, issue 3, 1999, pp. 285-294

[4] *S. Marzouk, F. Rachdi, M. Fourati, J. Bouaziz,* "Synthesis and grafting of silica aerogels", Coll. Surf. A: Phys. Eng. Asp., **vol. 234**, issues 1-3, 2004, pp. 109-116

[5] *C.R. Silva, S. Bachmann, R. Robelo Schefer, K. Albert, I.C. Sales Fontes Jardim, C. Airoldi,* "Preparation of a new C_{18} stationary phase containing embedded urea groups for use in high-performance liquid chromatography"**,** Journal of Chromatography A, **vol. 948**, issues 1-2, 2002, pp. 85-95

[6] *C.R. Silva, I.C. Fontes Jardim, C. Airoldi,* "Development of new urea-functionalized silica stationary phases: Characterization and chromatographic performance ", Journal of Chromatography A, **vol. 913**, issues 1-2, 2001, pp. 65-73

[7] *C.R. Silva, I.C. Fontes Jardim, C. Airoldi,* "Evaluation of the applicability and the stability of a C_{18} stationary phase containing embedded urea groups"*,* Journal of Chromatography A, **vol. 987**, issues 1-2, 2003, pp. 139-146

[8] *C.R. Silva, I.C. Sales Fontes Jardim, C. Airoldi,* "New generation of sterically protected C_{18} stationary phases containing embedded urea groups for use in high-performance liquid chromatography"*,* Journal of Chromatography A, **vol. 987**, issues 1-2, 2003, pp. 127-138

[9] *M. Klotz, A. Ayral, C. Guizard, L. Cot,* **"**Synthesis conditions for hexagonal mesoporous silica layers"**,** J. Mat. Chem., **vol. 10**, 2000, pp. 663-669

[10] *M. Ogawa, "*Formation of Novel Oriented Transparent Films of Layered Silica-Surfactant Nanocomposites"*,* J. Am. Chem. Soc., **vol. 116**, issue 17, 1994, pp. 7941-7942

[11] *M. Ogawa*, „Incorporation of Pyrene into an Oriented Transparent Film of Layered Silica-Hexadecyltrimethylammonium Bromide Nanocomposite", Langmuir, **vol. 11**, issue 12, 1995**,** pp. 4639–4641

[12] *M. Ogawa,* „A simple sol–gel route for the preparation of silica–surfactant mesostructured materials", Chem. Commun., 1996, pp. 1149 - 1150

[13] *M. Ogawa*, „Preparation of Layered Silica−Dialkyldimethylammonium Bromide Nanocomposites"**,** Langmuir, **vol. 13**, issue 6, 1997**,** pp. 1853-1855

[14] *M. Ogawa, T. Igarashi, K. Kuroda*, „Preparation of Transparent Silica-Surfactant Nanocomposite Films with Controlled Microstructures", Bull. Chem. Soc. Jpn., **vol. 70**, no. 11, 1997, pp. 2833-2837

[15] *Y. Lu, R. Gangull, C.A. Drewien, M.T. Anderson, C.J. Brinker, W. Gong, Y. Guo, H. Soyez, B. Dunn, M.H. Huang, J.I. Zink*, **„**Continuous formation of supported cubic and hexagonal mesoporous films by sol–gel dip-coating", Nature**, vol. 389,** 1997, pp. 364-368

[16] *M.T. Anderson, J.E. Martin, J.G. Odinek, P.P. Newcomer, J.P. Wilcoxon*, "Monolithic periodic mesoporous silica gels", Microporous Mater., **vol. 13**, 1997, pp. 10-16

[17] *J.E. Martin, M.T. Anderson, J.G. Odinek, P.P. Newcomer*, "Synthesis of Periodic Mesoporous Silica Thin Films", Langmuir, **vol. 13**, issue 15, 1997, pp. 4133–4141

[18] *A. Ayral, C. Balzer, T. Dabadie, C. Guizard, A. Julbe*, "Sol-gel derived silica membranes with tailored microporous structures", Catal. Today*,* **vol. 25**, issues 3-4, 1995, pp. 219-224

[19] *T. Dabadie, A. Ayral, C. Guizard, L. Cot, P. Lacan*, "Synthesis and characterization of inorganic gels in a lyotropic liquid crystal medium. Part 2.—Synthesis of silica gels in lyotropic crystal phases obtained from cationic surfactants**",** J. Mater. Chem., **vol. 6**, issue 11, 1996, pp. 1789-1794

[20] *M. Klotz, N. Indrissi-Kandri, A. Ayral, C. Guizard*, "Porous oxide thin layers using mesophase templating", Mat. Res. Soc. Symp. Proc., **vol. 628**, 2000, CC7.4.1

[21] *D. Grosso, F. Boboneau, P.A. Albouy, H. Amenitsch, A.R. Balkenende, A. Brunet-Bruneau, J.Rivory,* "An in Situ Study of Mesostructured CTAB−Silica Film Formation during Dip Coating Using Time-Resolved SAXS and Interferometry Measurements", Chem. Mater., **vol. 14,** issue 2, 2002, pp. 931-939

[22] *C.A. Peter, Alberius K.L. Frindell, R.C. Hayward, E.J. Kramer, G.D. Stucky, B.F. Chmelka,* "General Predictive Syntheses of Cubic, Hexagonal, and Lamellar Silica and Titania Mesostructured Thin Films", Chem. Mater., **vol. 14**, issue 8, 2002, pp. 3284–3294

[23] *N. Kitazawa, H. Namba, M. Aono, Y. Watanabe*, "Sol–gel derived mesoporous silica films using amphiphilic triblock copolymers", J. Non-Crystalline Solids, **vol. 332**, issues 1-3, 2003, pp. 199-206

[24] *M.C. Goncavalves, G.S. Attard*, "Nanostructured mesoporous silica films", Rev. Adv. Mater. Sci., **vol. 4**, no. 2, 2003, pp. 147-164

[25] *B. L. Newalkar, S. Komarneni,* "Synthesis and Characterization of Microporous Silica Prepared with Sodium Silicate and Organosilane Compounds **",** J.Sol-Gel Sci.Tech., **vol. 18**, issue 3, 2000, pp. 191-198

[26] *M. Klotz, A. Ayral, C. Guizard, L. Cot*, "Tailoring of the Porosity in Sol-Gel Derived Silica Thin Layers ", Bull. Korean Chem. Soc., **vol. 20**, no. 8, 1999, pp. 879-884

[27] *T.L. Barton, L.M. Bull, W.G. Klemperer, D.A. Loy, B. McEnaney, M.Misono, P.A. Monson, G. Pez, G. Scherer, J. Vartuli, O. Yaghi*, "Tailored Porous Materials", Chem. Mater., **vol. 11,** issue 10, 1999, pp. 2633-2656

[28] *D. Grosso, A. R. Balkenende, P. A. Albouy, A. Ayral, H. Amenitsch, F. Boboneau, "*Two-Dimensional Hexagonal Mesoporous Silica Thin Films Prepared from Block Copolymers: Detailed Characterization and Formation Mechanism", Chem. Mater., **vol. 13**, issue 5, 2001, pp. 1848-1856

[29] *P.A. Jal, M. Sudarshan, A. Saha, S. Patel, B.K. Mishra*, "Synthesis and characterization of nanosilica prepared by precipitation method", Coll.Surf.A: Phys.Chem.Asp., **vol. 240**, issues 1-3, 2004, pp. 173-178

[30] *H. J. Mathieu*, "Bioengineered material surfaces for medical applications ", Surface Interface Anal., **vol. 32**, issue 1, 2001, pp. 3-9

[31] *D.Y. Kwok,* "Measuring and interpreting contact angles: a complex issue", Coll. Surf. A: Phys. Eng. Asp., **vol. 142**, issues. 2-3, 1998, pp. 219-235

[32] *A.R. Venkateswara,* "Hydrophobic properties of TMOS/TMES-based silica aerogels", Mat. Res. Bull., **vol. 37**, issue 9, 2002, pp. 1667-1677

[33] *C. McDonagh, F. Sheridan; T. Butler, B.D. MacCraith*, "Characterisation of sol-gel-derived silica films", J. Non-Crystalline Solids, **vol. 194**, issues 1-2, 1996, pp. 72-77.